NÖHÜ Müh. Bilim. Derg. / NOHU J. Eng. Sci., 2025; 14(2), 722-731

Niğde Ömer Halisdemir Üniversitesi Mühendislik Bilimleri Dergisi
Niğde Ömer Halisdemir University Journal of Engineering Sciences

Araştırma makalesi / Research article

www.dergipark.org.tr/tr/pub/ngumuh / www.dergipark.org.tr/en/pub/ngumuh

# Experimental investigation of the behavior of unreinforced masonry structures under horizontal loads as defined in TBDY-2018

# TBDY-2018'de belirtilen yığma yapı türlerinden donatısız yığma yapıların yatay yükler etkisi altındaki davranışlarının deneysel olarak incelenmesi

**Mehmet Orhan[1,*], M. Sami Döndüren[2]**

[1] Selçuk University, Department of Construction, 42130, Konya, Türkiye
[2] Konya Technical University, Engineering and Natural Sciences Faculty, Civil Engineering Department, 42130, Konya, Türkiye

**Abstract**

Masonry structures constitute a significant portion of the building stock in Turkey and are commonly used, particularly along the East Anatolian, North Anatolian, and Western Aegean fault lines. These structures are often preferred for economic reasons; however, due to inadequate material quality and construction techniques, they present a considerable seismic risk. Among the various masonry types defined in the Turkish Building Earthquake Code (TBDY 2018), unreinforced masonry structures were experimentally investigated in this study. A full-scale, single-story, single-span unreinforced masonry specimen was constructed in a laboratory environment and subjected to reversed cyclic loading tests. The loading procedure of the experiment was conducted in a load-controlled manner up to the maximum load, and in a displacement-controlled manner after reaching the maximum load. At each stage of the experimental studies, the applied load and displacement values were recorded through a computer. The sizes, thicknesses, and locations of the cracks formed in the structure were carefully monitored and marked on the structure, and the damage state was determined in detail. This study aimed to evaluate the seismic performance of unreinforced masonry structures, focusing on crack formation regions under tensile and compressive loads. The findings reveal that cracks predominantly form around window openings, and unreinforced masonry structures exhibit brittle behavior. Consequently, the study highlights the importance of investigating other types of masonry structures and conducting comparative analytical analyses to understand their performance comprehensively.

**Keywords:** Experimental model analysis, Masonry structures, TBDY-2018 (Turkish Building Earthquake Code), Types of masonry structures, Unreinforced masonry structure, Seismic performance

**Öz**

Yığma yapılar, Türkiye'deki yapı stoğunun önemli bir bölümünü oluşturmakta ve özellikle Doğu Anadolu, Kuzey Anadolu ve Batı Ege fay hatları boyunca yaygın olarak kullanılmaktadır. Genellikle ekonomik nedenlerle tercih edilen bu yapılar, malzeme kalitesi ve inşaat tekniklerinin yetersizliği nedeniyle depreme karşı risk taşımaktadır. Türkiye Bina Deprem Yönetmeliği (TBDY 2018) kapsamında tanımlanan farklı yığma yapı türleri arasında yer alan donatısız yığma yapılar, bu çalışmada deneysel olarak incelenmiştir. Çalışmada, 1/1 ölçekli, tek katlı ve tek açıklıklı donatısız yığma yapı numunesi laboratuvar ortamında üretilmiş ve tersinir yükleme testine tabi tutulmuştur. Deney yükleme prosedürü, maksimum yüke kadar yük kontrollü, maksimum yükten sonra ise deplasman kontrollü olarak gerçekleştirilmiştir. Deneysel çalışmaların her aşamasında, uygulanan yük ve deplasman değerleri bilgisayar aracılığıyla kaydedilmiştir. Yapıda oluşan çatlakların boyutları, kalınlıkları ve yapıda bulundukları konumlar dikkatle gözlemlenmiş ve yapıya işaretlenerek hasar durumu detaylı bir şekilde belirlenmiştir. Bu çalışma, donatısız yığma yapıların deprem performansını incelemiş olup çekme ve itme yükleri etkisi altındaki binadaki çatlak oluşum bölgeleri gözlemlenmiştir. Sonuç olarak, donatısız yığma yapıların pencere çevresinde çatlaklarının oluştuğu ve gevrek bir davranış sergilediği, bu nedenle diğer yığma yapı türlerinin incelenmesi ve analitik olarak karşılaştırılmasının önem taşıdığı anlaşılmaktadır.

**Anahtar kelimeler:** Deneysel model analiz, Yığma yapılar, TBDY-2018, Yığma yapı türleri, Donatısız yığma yapı, sismik performans

## 1 Introduction

Turkey is located on one of the most seismically active regions in the world, as illustrated in Figure 1, which presents the seismic hazard map of the country. A significant portion of Turkey's population resides in areas with high seismic risk.

This situation increases the loss of life and property caused by earthquakes, thus making it necessary to take precautions to reduce the earthquake risk. One of the primary factors contributing to building collapses in Turkey is

* Sorumlu yazar / Corresponding author, e-posta / e-mail: mehmet.orhan@selcuk.edu.tr (M. Orhan)
Geliş / Received: 03.01.2025 Kabul / Accepted: 19.03.2025 Yayımlanma / Published: 15.04.2025
doi: 10.28948/ngmuh.1612998

inadequate design and poor construction quality in response to seismic loads. To address these losses, the Turkish Building Earthquake Code 2018 (TBDY-2018) was enacted.

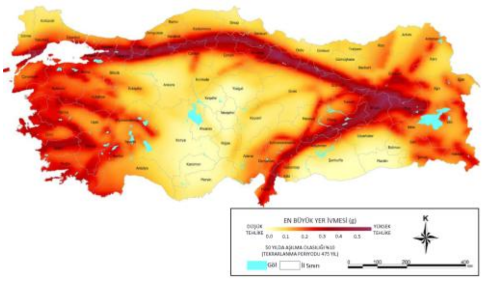

**Figure 1.** The seismic hazard map of Turkey [1]

TBDY-2018 provides criteria for designing earthquake-resistant structures, including masonry buildings. Masonry structures, constructed using materials such as stone, brick, and concrete blocks, are notable for their ability to bear both vertical and horizontal loads. These structures are particularly prevalent in rural areas and historical buildings, offering advantages such as low cost and simple construction techniques. Furthermore, masonry structures hold cultural significance as they reflect the architectural and engineering knowledge of past eras.

In this study, unreinforced masonry structures, as defined under TBDY-2018, were investigated for their behavior under different loading conditions. Experimental tests were conducted on a full-scale, single-story, single-span unreinforced masonry specimen in a laboratory environment. The structures were subjected to reversed cyclic loads.

The primary aim of this study is to experimentally examine the behavior of masonry structures under seismic effects and assess their damage states.

The literature highlights several experimental academic studies focusing on the seismic behavior of masonry structures. For instance, Saberi [2], investigated the seismic behavior of masonry walls with door openings having a height-to-width ratio greater than one, employing quasi-static testing methods to analyze the influence of this ratio on seismic performance. Döndüren [3], constructed two full-scale masonry wall prototypes with identical geometric properties in a laboratory setting; one was built with normal mortar, while the other used Sikalatex-enhanced mortar, and both were subjected to compression tests. Döndüren and Kollu [4], analyzed the damage and collapse causes of masonry structures during earthquakes in Turkey over the past 15 years, using photographs to support their findings, and proposed solutions for mitigating damage in rural areas. Yıldızoğlu, Can, and Tayfur [5], examined the material properties and existing issues of the Korkut Ata High School in Bayburt using the StatiCAD-Masonry program, evaluating its performance under the 2007 Earthquake Code and the 2013 Risky Buildings Regulation. Bahadır and Balık [6], developed 1/6 scale, single-story, three-bay masonry prototypes using various wall bonding techniques and subjected these prototypes to dynamic tests on a shaking table, with displacement measurements captured through image processing and acceleration data obtained using accelerometers. García, Jiménez-Pacheco, and Ulloa [7], analyzed the seismic resilience of brick structures using an experimental damage model, validating this model with real-life examples from Cuenca, Ecuador. Kanit R., Erdal M., and Can O. [8], experimentally investigated the behavior of load-bearing masonry walls under out-of-plane loads. The effects of different material types and wall geometries on load-bearing capacity and cracking behavior were evaluated, and design recommendations were provided based on the results. [9], Kıpçak F. and Erdil Barış, in their study, they experimentally and analytically examined the out-of-plane behavior of brick masonry walls, demonstrating that side walls increase stiffness and lateral load capacity, while door and window openings reduce stiffness, leading to earlier and more brittle failure.

These studies significantly contribute to understanding and improving the seismic behavior of masonry structures under varying conditions.

## 2 Materials and methods

As part of this study, a single-story, full-scale (1:1) unreinforced masonry building specimen (S1) with dimensions of 3.2 m × 3.3 m × 3.0 m was constructed. This specimen was experimentally investigated under the influence of reversed and repeated loads.

Loading Process: Reversed cyclic loads were applied to the setup using a hydraulic loading system. The resulting damage under the applied loads were marked and visually observed on the building wall's surface.

Displacement Measurement: Displacement values were recorded using displacement gauge and a data acquisition system.

Test Environment: All experiments were conducted at the Structural and Earthquake Laboratory of the Department of Civil Engineering, Faculty of Engineering and Natural Sciences, Konya Technical University.

### *2.1 General characteristics of the specimen designed as an unreinforced masonry building*

The unreinforced masonry building setup used in the experimental study was prepared in accordance with the minimum requirements specified in the *Turkish Building Earthquake Code 2018 (TBDY 2018). The architectural plan of the building is presented in Figure 2.

Materials and Geometry: The materials and geometric properties used in the construction of the setup were designed in compliance with the standards outlined in TBDY 2018.

In this study, the experimental specimen was constructed using binding mortar and load-bearing masonry bricks. The window openings measure 100 cm × 100 cm each (two windows), and the door opening measures 100 cm in width and 200 cm in height. The door openings begin at the foundation level, while the window openings are positioned 100 cm above the foundation level. Displacement transducers were placed at the corner points of the specimen, and the loading system was arranged at the top floor level of the rear facade.

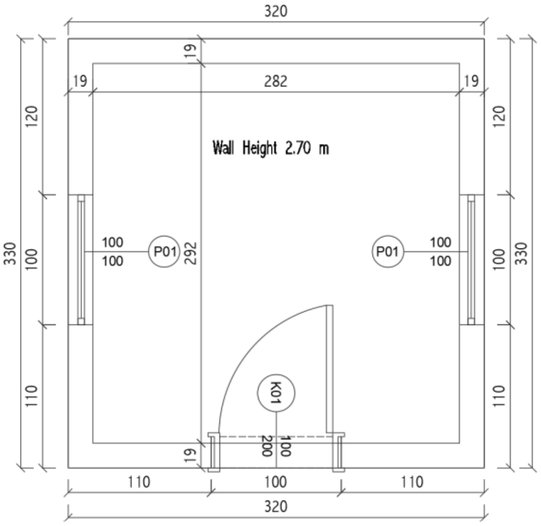


**Figure 2.** The architectural plan of the unreinforced masonry building

The detailed views and geometric dimensions of the specimen's left, right, front, and rear facades are presented in Figure 3.

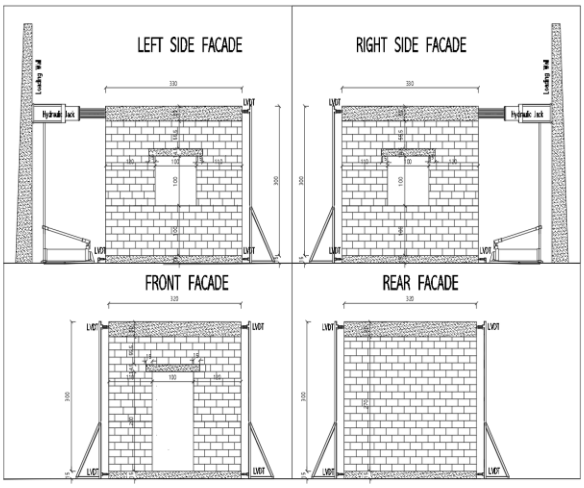


**Figure 3.** The views of the masonry test specimen

*2.1.1 Materials used in the construction of the unreinforced masonry building specimen and compression strength tests*

Load-bearing bricks with dimensions of 190 × 290 × 135 mm, compliant with the standards outlined in TBDY 2018, were used in the construction of the masonry walls. To ensure that the bricks met the minimum quality requirements, three samples were prepared and subjected to compression strength tests. The compressive strengths of the bricks were calculated by excluding the void areas of the bricks. The brick void ratio was calculated as 0.52 in Figure 4.

The compression strength results of the brick samples are presented in Table 1, and the average compression strength value was used for analysis.

**Table 1.** Results of the brick compression strength test

| Number No | Compressive Strength (MPa) | Average (MPa) |
|---|---|---|
| 1 | 5.15 | |
| 2 | 5.32 | 5.14 |
| 3 | 4.94 | |

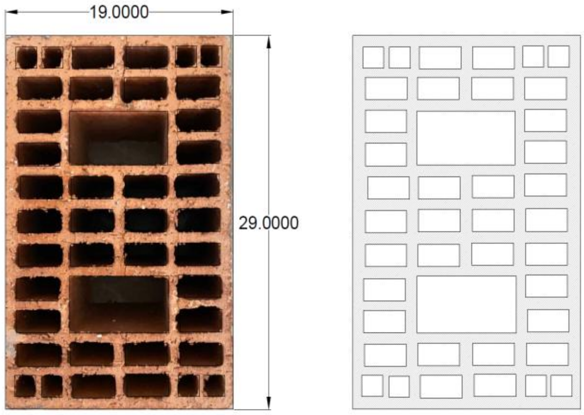


**Figure 4.** Dimensions of the test brick.

Table 2 presents the compressive strength results of the mortar samples used in the compressive strength test of the walls of the unreinforced masonry specimen. To test the strength of the mortar used in the unreinforced masonry building specimen, three cube samples with dimensions of 15x15x15 cm were taken. The samples were cured in water for 28 days in accordance with standard procedures and then tested for compressive strength at the Material Laboratory of Konya Technical University.

The compressive strength values obtained from tests conducted on brick and mortar materials in accordance with TS EN 772-1 and TS EN 1015-11 standards are used for determination [10].

**Table 2.** Compressive strength of mortar in unreinforced masonry walls

| Number No | Compressive Strength (MPa) | Average (MPa) |
|---|---|---|
| 1 | 9.41 | |
| 2 | 10.19 | 10.40 |
| 3 | 11.59 | |

The concrete class of reinforced concrete components used in unreinforced, reinforced, confined masonry buildings, and reinforced panel system buildings must be at least C25 [11].

To determine the mechanical properties of the concrete used in foundations, slabs, and horizontal beams, three cube samples with dimensions of 15×15×15 cm were taken during the concrete casting process.

Table 3 provides a detailed presentation of the samples used in the compressive strength tests of the concrete in the foundations, slabs, and horizontal beams of the unreinforced masonry walls.

**Table 3.** Compressive strength of concrete samples used in the experiments

| | Building Foundation | |
|---|---|---|
| Number No | Compressive Strength (MPa) | Average (MPa) |
| 1 | 26.41 | |
| 2 | 24.78 | 26.26 |
| 3 | 27.58 | |
| | Floor, Horizontal Beams | |
| Number No | Compressive Strength (MPa) | Average (MPa) |
| 1 | 25.15 | |
| 2 | 23.98 | 25.51 |
| 3 | 27.41 | |

### 2.1.2 *Dimensions and technical specifications of the test specimen's foundation*

The foundation used in the unreinforced test specimen was designed with dimensions of 320 cm×330 cm and a height of 15 cm, as shown in Figure 5, ensuring a rigid diaphragm property.

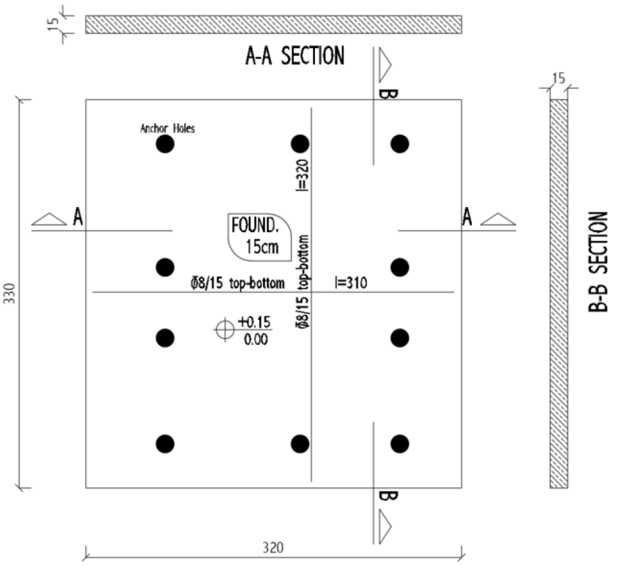


**Figure 5.** Technical drawing of the test specimen's foundation plan

After the completion of formwork and reinforcement works, ready-mix concrete of class C25 was ordered, and the concrete was cast. The concrete was placed using a concrete pump, and images of the process before and after the casting are presented in Figure 6.

The reinforcement and formwork plan for the horizontal beams is shown in Figure 7. B420C ribbed steel reinforcements were used in the horizontal beams. The reinforcements were tied with binding wire, and longitudinal reinforcements of 6Ø12 and stirrups of Ø8 spaced at 150 mm intervals were placed.

**Figure 6.** Foundation concrete casting for test specimens

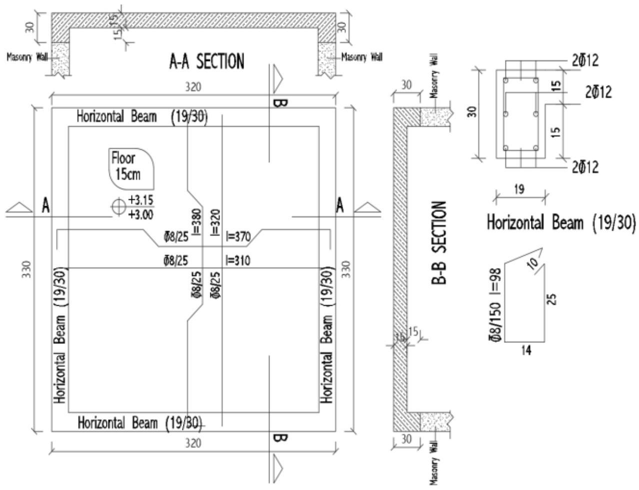


**Figure 7.** Formwork and reinforcement plan for the floor and horizontal beams of the unreinforced masonry building

After completing the reinforcement assembly, the concrete casting process was initiated. Concrete of class C25 was placed on the floor using a concrete pump. The concrete casting process is illustrated in Figure 8.

**Figure 8.** Concrete casting process

The formwork was removed after a 15-day curing period to allow the concrete to set. To enhance the visibility of cracks and fractures during analysis, the surfaces were painted with white paint, as shown in Figure 9.


**Figure 9.** Appearance of the unreinforced test specimen painted in white

### 2.1.3 *Experimental setup for the unreinforced masonry building*

In the experiments, load measurements were conducted using a single load cell, while displacement measurements were obtained using 12 linear variable displacement gauge (LVDTs). To enhance the precision of the LVDTs, 15 cm × 15 cm glass plates were cut and fixed at the contact points on the specimen using silicone. Data from the load cell and LVDTs were transmitted via cables to a data acquisition system.

The measurements recorded by the data acquisition system were transferred to a computer through a device known as a gateway. The system comprised 13 channels in total, including 12 LVDTs (4 of which were positioned at the foundation) and 1 load measurement channel (Channel 8) in Figure 10.

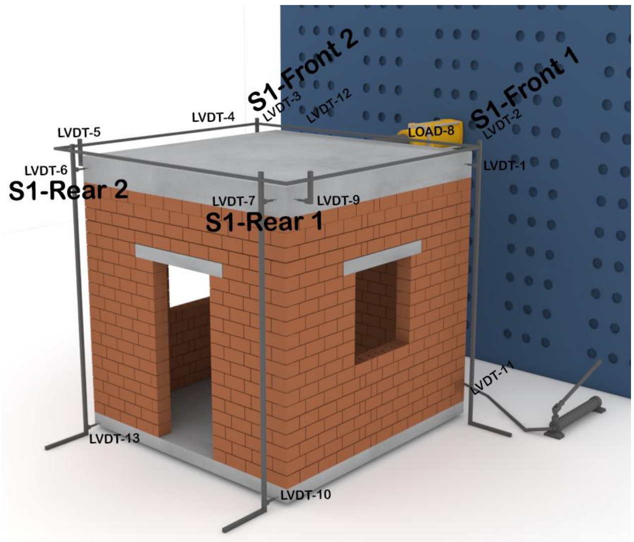


**Figure 10.** Naming of the elements in the unreinforced test specimen (S1)

The data transferred to the computer were analyzed in real-time using specialized software, enabling the simultaneous generation of desired graphs during the experiments.

LVDTs and the load cell data were utilized to evaluate the load-deformation relationships and mechanical performance of the specimens. Graphs were prepared for each specimen to visualize the experimental results, with detailed attention to the data processing methods and analysis steps involved in their creation. This approach to data processing and graphical representation served as a fundamental method for assessing the experimental outcomes.

## 3 Findings and Discussion

The pre-test images of the S1 test specimen are shown in Figure 11.


**Figure 11.** Pre-test appearance of the S1 test specimen

The loading procedure of the experiment was conducted in a load-controlled manner up to the maximum load, and in a displacement-controlled manner after reaching the maximum load. Since the reinforced masonry structures to be examined in future studies, as mentioned at the end of the article, are expected to exhibit behavior similar to that of reinforced concrete structures, the loading procedure was designed to be consistent with the procedures used for reinforced concrete structures. The loading procedure for reinforced concrete structures is generally performed in a load-controlled manner up to the maximum load, followed by a displacement-controlled manner after the maximum load. To ensure consistency in the comparison with the reinforced masonry structure in this study, the same loading procedure was applied.

The loading history applied during the tests conducted on the S1 specimen and the resulting displacement values are presented in Table 4.

The horizontal load-peak displacement hysteresis curves obtained from the front and rear faces of the S1 test specimen are presented and analyzed in detail in the results section. These graphs comprehensively illustrate the mechanical behavior and performance of the specimen under loading conditions (Figure 12).

**Table 4.** Horizontal loads applied to the s1 test specimen and the resulting displacements

| S1 CYCLES | S1-Front 1 | S1-Front 2 | S1-Rear 2 | S1-Rear 1 | Horizontal Load (kN) |
|---|---|---|---|---|---|
| | LVDT-2- Front (mm) | LVDT-3- Front (mm) | LVDT-6- Rear 2 (mm) | LVDT-7- Rear 1 (mm) | |
| -8 | 4.18 | 0.33 | -2.55 | -4.26 | -46.99 |
| -7 | 5.40 | 1.51 | -3.73 | -4.23 | -59.68 |
| -6 | 2.59 | 0.89 | -1.38 | -2.07 | -55.65 |
| -5 | 1.66 | 2.29 | -1.43 | -2.23 | -49.13 |
| -4 | 0.92 | 1.26 | -0.84 | -1.01 | -40.28 |
| -3 | 0.74 | 1.02 | -0.68 | -0.76 | -31.11 |
| -2 | 0.46 | 0.69 | -0.42 | -0.44 | -21.00 |
| -1 | 0.18 | 0.38 | -0.17 | -0.14 | -10.73 |
| 0 | 0.00 | 0.00 | 0.00 | 0.00 | 0.00 |
| +1 | -0.12 | -0.15 | -0.12 | -0.13 | 9.46 |
| +2 | -0.35 | -1.15 | 0.33 | 0.36 | 21.90 |
| +3 | -1.10 | -2.03 | 1.11 | 1.11 | 29.82 |
| +4 | -2.39 | -3.48 | 2.43 | 1.09 | 38.68 |
| +5 | -4.12 | -5.04 | 4.24 | 2.45 | 38.61 |
| +6 | -10.33 | -10.04 | 10.45 | 6.98 | 32.83 |
| +7 | -12.00 | -13.88 | 11.66 | 10.53 | 26.14 |
| +8 | -17.53 | -19.40 | 17.18 | 14.40 | 22.62 |

The maximum horizontal load generated in the push and pull directions and the corresponding displacement values are presented in Table 4. The structure carried less horizontal load in the push direction. This indicates that brittle building systems such as masonry have a higher load-bearing capacity in the compression direction, while the load-bearing capacity in the other direction is not significantly affected. Since the unreinforced specimen exhibited brittle behavior, its stiffness was found to be high. As the load increased, the amount of damage in the unreinforced specimen also increased, leading to higher displacement values, which in turn resulted in a reduction in stiffness during subsequent cycles.

In the loading protocol applied to the S1 test specimen, no movement was observed in the foundation plane. A total of ±8 cycles of loading were applied during the experiment, transitioning from load-controlled to displacement-controlled loading at the end of the process. While no cracks were observed during the first three cycles, the first crack appeared during the +4th cycle (Figure 13).

During this cycle, the total horizontal load applied to the specimen reached a maximum of 38.68 kN, followed by a reduction in the pushing load. The displacement values measured during the +4th cycle were recorded as 2.39 mm (S1-Front 1) and 3.48 mm (S1-Front 2) on the front face and 1.09 mm (S1-Rear 1) and 2.43 mm (S1-Rear 2) on the rear face (Table 6).

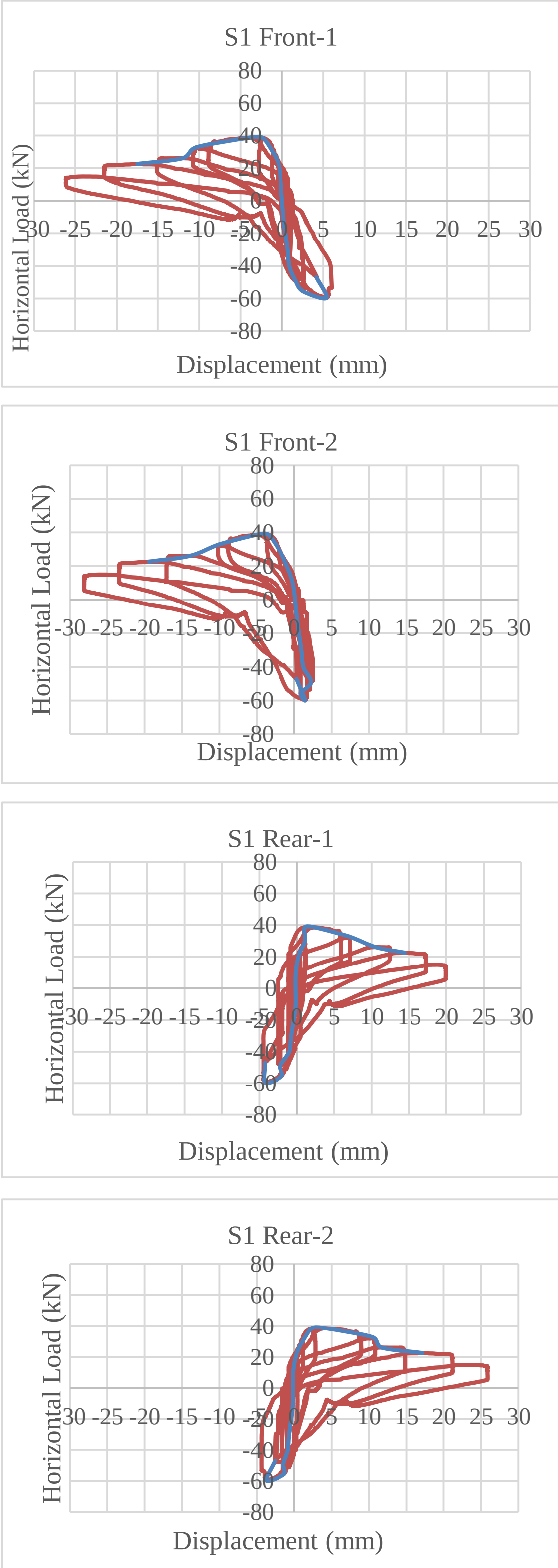


**Figure 12.** Cyclic hysteresis curves of horizontal load-displacement for the S1 test


**Figure 13.** General appearance after the 4th cycle

In the -7th cycle, the maximum horizontal load resistance of the specimen was measured as 59.68 kN. During this cycle, the displacements were recorded as 5.40 mm (S1-Front 1) and 1.51 mm (S1-Front 2) on the front face and 4.23 mm (S1-Rear 1) and 3.73 mm (S1-Rear 2) on the rear face. Crack formations were observed around the windows, including shear cracks inclined at approximately 45° and horizontal sliding cracks in the upper and lower regions of the windows.

The loading protocol continued during the 7th cycle, and the specimen was loaded up to a crack level of 30 mm. This process was closely monitored to determine the reduction in the load-bearing capacity and the extent of damage to the specimen (Figure 14).


**Figure 14.** General appearance after the 7th cycle

After the 7th cycle, diagonal (shear) cracks were observed, particularly in areas near the edges of the windows and corners (Figure 15).

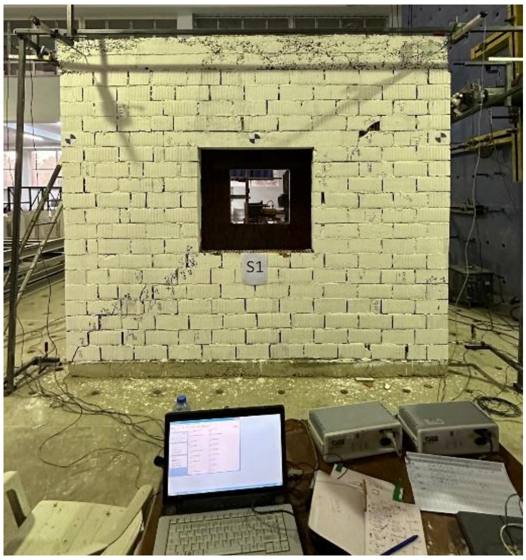


**Figure 15.** General appearance after completion of all cycles

The types of cracks that may occur in masonry structures after an earthquake are shown in Figure 16.

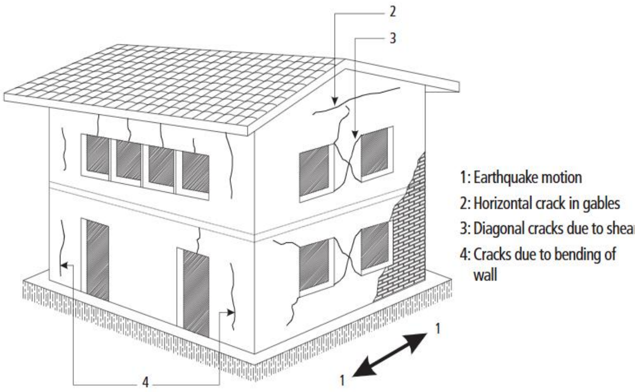


**Figure 16.** Types of cracks that may occur in masonry structures after an earthquake [12].

Figure 17 details the types of fractures that occur in masonry walls under loads parallel to the horizontal joints. These include cracks along the bricks (Figure 17a), shear cracks passing through the joints (Figure 17b), crushing at the wall toes (Figure 17c), and rocking of load-bearing walls due to separation from the floors (Figure 17d) [13].

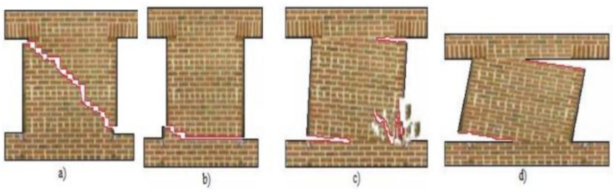


**Figure 17.** Failure modes in masonry walls under the effect of loads parallel to horizontal joints [13].

The cracks formed after the S1 test were analyzed by mapping them on the left side of the specimen. Diagonal cracks in the specimen initiated from the edges of the windows and propagated upward and downward at a 45° angle, being classified as shear cracks.

The concentration of cracks around window and door openings indicates that these regions are structurally weak due to stress concentration. Horizontally propagating cracks in areas with mortar infill typically suggest damage resulting from friction or weak connections under horizontal loads.

The accumulation of dense cracks around the windows and in the lower sections of the walls reveals that the load was more concentrated in these areas, identifying them as critical weak points in the structure (Figure 14).

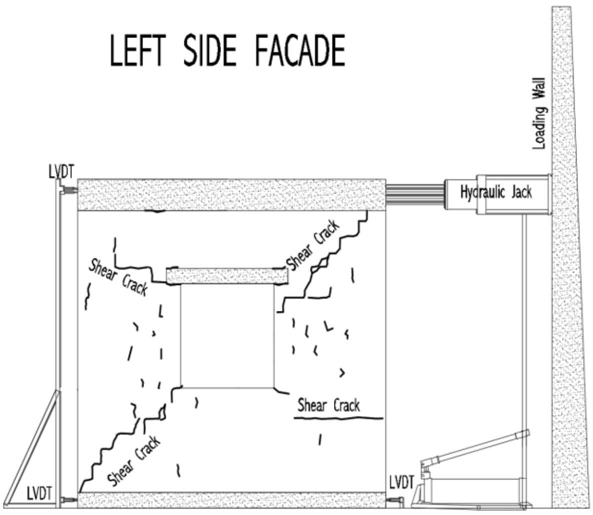


**Figure 14.** Appearance of the cracks on the left side facade of the s1 test specimen after the experiment

Based on the data obtained from the hysteresis curve of the S1 specimen, envelope curves were generated using the maximum load values measured in each cycle and the corresponding displacement values (Figure 15).

As shown in Figure 15, the unreinforced masonry structure exhibited brittle behavior, indicating that while the building system has a higher load-bearing capacity in the compression direction, it has no significant effect on the load-bearing capacity in the opposite direction.

The maximum load values in the tension and compression directions, along with the corresponding displacement values, are presented in Table 6.

In each experimental cycle, the cyclic stiffness was calculated by taking the ratio of the maximum horizontal load to the corresponding horizontal displacement (Figure 16).

In the graph, the stiffness values obtained from the push cycles are presented on the right side, while the values from the pull cycles are shown on the left side. These calculations were carried out to evaluate the stiffness variations exhibited by the specimen in each cycle and to analyze its mechanical behavior in detail.

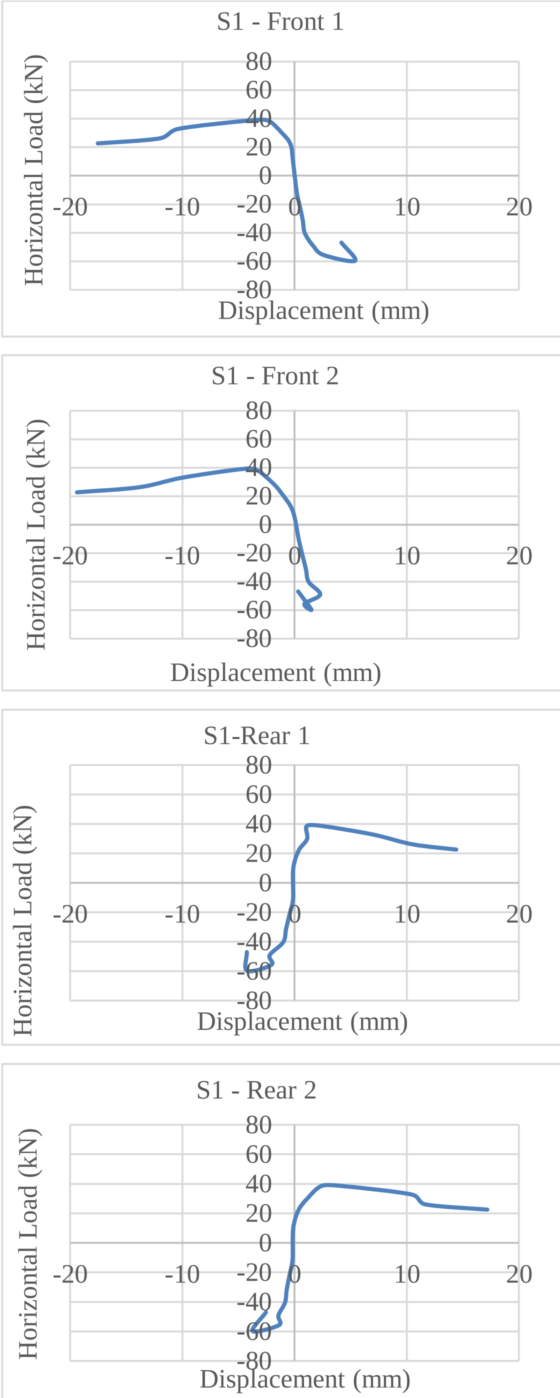


**Figure 15.** Horizontal load-displacement graphs of the S1 test specimen

**Table 6.** Displacement values corresponding to the maximum loads in tensile and compressive for the S1 test

| Maximum Load | | Peak Displacement at Maximum Load (mm) | | | | | |
|---|---|---|---|---|---|---|---|
| | | Front 1 | | Rear 1 | | Rear 2 | |
| Tensile (T) | Compressive (C) | T | C | T | C | T | C |
| -59.7 | 38.7 | -5.4 | 2.4 | -4.2 | 1.1 | -3.7 | 2.4 |

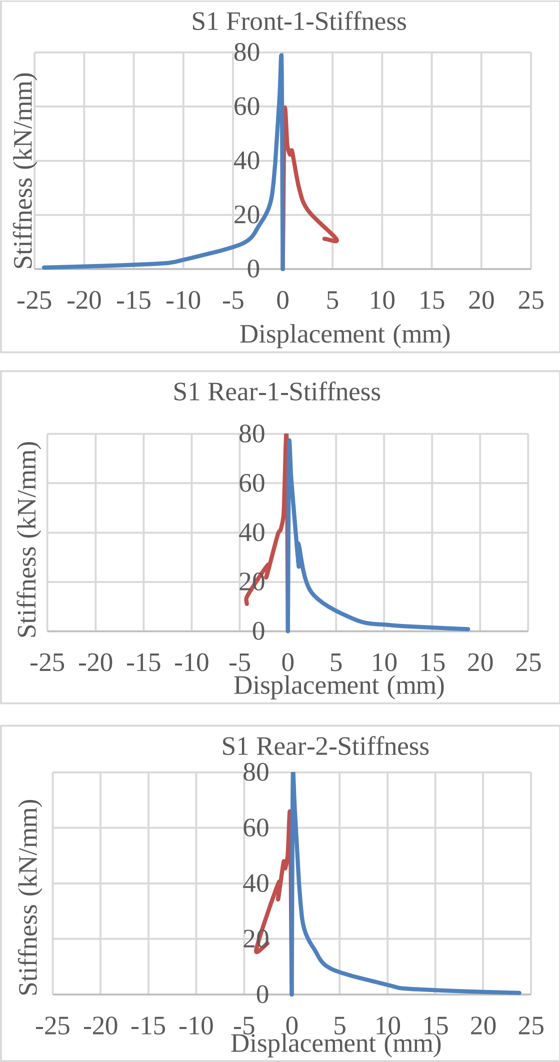


**Figure 16.** Stiffness degradation curve of the S1 test

## 4 Conclusions

When a lateral load, such as seismic forces, is applied to structures, they initially exhibit rigid behavior rather than ductile behavior. The initial stiffness observed in this phase indicates the structures' ability to undergo displacements under low loads.

In the case of the unreinforced specimen, as the load increased, the amount of damage also increased, leading to higher displacement values. As a result, stiffness decreased in subsequent cycles. It was observed that these structures exhibited brittle behavior, with a rapid reduction in stiffness under horizontal loading and inadequate performance in the tensile direction.

In the experimental studies, fractures and cracks were formed in the brick and mortar elements. The stress concentrations around the window and door openings indicate that these regions are weak points in masonry buildings. Such stress concentrations can lead to the initiation of cracks or material fatigue over time. The stress concentrations around the openings emerge as critical regions in terms of structural integrity.

Research on reinforced, confined, and reinforced panel masonry buildings, as defined in TBDY-2018, is essential for comparing with existing studies and evaluating the performance of these structures.

Design and material improvements can be made by optimizing the reinforcement and adding strengthening elements at the edges of windows and doors to reduce stress concentrations.

## Acknowledgement

This study is derived from the doctoral thesis titled "Experimental and Analytical Investigation of the Behavior of Masonry Structures Under Horizontal Loads as Defined in TBDY-2018" prepared by Lecturer Mehmet Orhan. In the study, the behavior of reinforced masonry structures under lateral loads will be comprehensively examined using both experimental and analytical methods. While the experimental studies will be conducted in a laboratory environment, the analytical analyses will be performed using ANSYS software. The experimental and analytical data obtained will be evaluated comparatively, and recommendations will be provided regarding the practical challenges and advantages of the design criteria specified in the regulations, focusing on the cost and applicability of these structures. Thus, the study aims to make a significant contribution to existing literature. The doctoral thesis has been supported by the Scientific Research Projects (BAP) Coordination Unit of Konya Technical University.

## Conflict of interest

The authors declare that there is no conflict of interest.

**Similarity rate (ithenticate):** %14

## References

[1] AFAD, Seismic Hazard Map Summary Report, Jan. 2, 2018. [Online]. Available: https://tdth.afad.gov.tr/TDTH/ozetRapor.xhtml [Accessed: Dec. 2, 2024].

[2] M. Saberi, Behavior of Masonry Buildings under Earthquake Loads, MSc thesis, Istanbul Technical University, 1998.

[3] M. S. Döndüren, Effect of Improved Mortar and Plaster on the Mechanical Behavior of Out-of-Plane Loaded Brick Walls, MSc thesis, Selçuk University, Institute of Science, 2008.

[4] M. S. Döndüren and M. S. Kollu, "Damages and Causes Observed in Masonry Buildings During Earthquakes in Turkey in the Last 15 Years," Selçuk Technical Journal, vol. 17, no. 2, pp. 59–70, 2018. [Online]. Available: http://sutod.selcuk.edu.tr/sutod/article/view/438.

[5] H. Yıldızoğlu, Ö. Can, and B. Tayfur, "Determination of Earthquake Performance in Masonry Buildings (Case Study of Bayburt Korkut Ata High School)," Gümüşhane University Journal of Science, vol. 8, no. 2, pp. 372–380, 2018. doi:10.17714/GUMUSFENBIL.380259.

[6] F. Bahadır and F. S. Balık, "Shake Table Tests of Prototype Masonry Buildings Constructed with

Different Wall Bond Patterns," Konya Journal of Engineering Sciences, vol. 9, no. 2, pp. 343–358, 2021. doi:10.36306/KONJES.837692.

[7] H. García, J. Jiménez-Pacheco, and J. Ulloa, "Effective Properties of Masonry Structures and Macro-Model Analysis with Experimental Verification," Results in Engineering, vol. 23, 102546, 2024. doi:10.1016/J.RINENG.2024.102546.

[8] R. Kanit, M. Erdal, and O. Can, "Assessing the Experimental Behaviour of Load-Bearing Masonry Walls Subjected to Out-of-Plane Loading," Scientific Research and Essays, vol. 5, no. 21, pp. 3336–3344, 2010.

[9] F. Kıpçak and B. Erdil, "Effect of Side Wall and Side Wall Opening on the Out-of-Plane Behavior of Masonry Structures," Niğde Ömer Halisdemir University Journal of Engineering Sciences, vol. 12, no. 3, pp. 853–860, 2023. doi:10.28948/ngumuh.1268912.

[10] Turkish Standards Institution, TS EN 772-1 and TS EN 1015-11, Standards Publication.

[11] Ministry of Interior Disaster and Emergency Management Authority (AFAD), Turkish Building Earthquake Code (TBDY), Ankara, Turkey, 2018.

[12] A. S. Arya, T. Boen, and Y. Ishiyama, Guidelines for Earthquake Resistant Non-Engineered Construction, UNESCO, 2014. [Online]. Available: https://unesdoc.unesco.org/ark:/48223/pf0000229059 [Accessed: Apr. 8, 2025].

[13] F. L. Moon, Seismic Strengthening of Low-Rise Unreinforced Masonry Structures with Flexible Diaphragms, PhD thesis, Georgia Institute of Technology, Dec. 11, 2003. [Online]. Available: http://hdl.handle.net/1853/5128 [Accessed: Apr. 8, 2025].